Adnan A.S. El khaldy*, Afef Janen, Alaa Abushanab and Ebony Stallworth

Synthesis, characterization, and antimicrobial activites of some dithiophosphate silane complexes

DOI 10.1515/mgmc-2015-0029
Received September 5, 2015; accepted September 19, 2016; previously published online November 5, 2016

Abstract: The compounds $MeCl_2Si[S_2P(OR)_2]$, $MeClSi[S_2POGO]_2$, and $MeSi[S_2P(OR)_2]_3$ (where R = Et, *n*-Pr, *i*-Pr, *i*-Bu, and Ph; G = $-CH_2CMe_2CH_2-$, $-CH_2CEt_2CH_2-$, and $-CMe_2CMe_2-$) have been prepared by reacting the sodium salt of the appropriate dithiophosphoric acid or the acid itself with $MeSiCl_3$ in 1:1, 1:2, and 1:3 molar ratios, in benzene, at reflux. These compounds are yellow oily liquids and soluble in common organic solvents. The molecular weight determination corresponds to monomers. The compounds have been characterized by elemental analysis and by ^{1}H, ^{13}C, ^{29}Si, and ^{31}P NMR spectroscopies. The ligands coordinate in a monodentate mode to the silicon atoms which in turn show a tetrahedral environment. Screening these complexes for their antibacterial activities gave positive results.

Keywords: dialkyl and alkylene dithiophosphates; dialkyl and alkylene dithiophosphates of methylsilane; methylsilane dithiophosphates.

Introduction

There has been a prodigious upsurge in the synthesis and elucidation of the structure of some metal complexes containing dithio-substituted ligands, such as dithiophosphates, xanthates, dithiocarbamates, and dithiocarboxylates (Cotero-Villegas et al., 2011; Petrus et al., 2011; García y García et al., 2012; Lutz et al., 2012; Kaub et al., 2014).

The stabilization of metals in high oxidation states, extensive electron transfer series and other such structural, magnetic, and spectroscopic properties have served to make 1,1-dithio complexes, especially the dithiophosphates, the focus of attention to sulfur donor ligand complexes. The dithiophosphates and the applications as anti-oxidant additives are extremely important in the oil- and petroleum industry. Particularly zinc dithiophosphates (Kim et al., 2010; Zhao et al., 2014) were used as a lubricant additive (anti-oxidant) for the past 70 years paving the way for new technology. Also worth mentioning is the use of such compounds as pesticides. O, O-dialkyl and alkylene dithiophosphoric acids possess the fragment (S = P-SH) and behave as versatile dithio ligands (Ma et al., 2010) forming a variety of complexes with transition (Rodina et al., 2015) and nontransition metals (Elkhaldy et al., 2011). The synthesis of organosilane (IV) dithiophosphate compounds provides model systems of interest because the presence of both biologically active organosilicon and dithiophosphate moieties in a single molecule could provide more powerful and lasting effects. It was thought worthwhile to undertake a detailed and systematic study of these type of complexes.

Results and discussion

Methylsilane of mixed chloro and tris O, O-dialkyl and alkylene dithiophosphate compounds are prepared in 85%–95% yields by the salt metathesis reactions of the corresponding sodium salts of dithiophosphoric acid with methyltrichlorosilane in 1:1, 1:2, and 1:3 molar ratios. These reactions are facile but to ensure completion reaction, solutions were heated at reflux with stirring for ~5 h in anhydrous benzene.

$$MeSiCl_3 + nNaS_2P(OR)_2 \rightarrow MeSi[S_2P(OR)_2]_nCl_{(3-n)} + (3-n)\ NaCl \text{ or}$$

$$MeSiCl_3 + nHS_2P(OR)_2 \rightarrow MeSi[S_2P(OR)_2]_nCl_{(3-n)} + (3-n)\ HCl$$

where R = Et, *n*-Pr, *i*-Pr, *i*-Bu and Ph, $n = 1, 2$, and 3

$$MeSiCl_3 + nNaS_2POGO \rightarrow MeSi[S_2POGO]_nCl_{(3-n)} + (3-n)NaCl \text{ or}$$

$$MeSiCl_3 + nHS_2POGO \rightarrow MeSi[S_2POGO]_nCl_{(3-n)} + (3-n)HCl$$

***Corresponding author: Adnan A.S. El khaldy,** Department of Physics, Chemistry and Mathematics, Alabama A&M University, Normal, AL 35762, USA, e-mail: adnan.elkhaldy@aamu.edu
Afef Janen and Ebony Stallworth: Department of Physics, Chemistry and Mathematics, Alabama A&M University, Normal, AL 35762, USA
Alaa Abushanab: Department of Chemistry, Al-Aqsa University, Gaza Strip, Palestine

where G = -$CH_2CMe_2CH_2$-, -$CH_2CEt_2CH_2$- and -CMe_2CMe_2-, $n = 1$, 2, and 3.

Alternatively, these compounds can be prepared in similar yields by the reaction of $MeSiCl_3$ with the corresponding dithiophosphoric acids (Table 1).

IR spectra

The infrared spectra of these O, O-dialkyl and alkylene dithiophosphate of silane compounds have been recorded in the region 4000–200 cm^{-1}. The IR bands were made on the basis of comparisons with the spectra of the dialkyl and alkylene dithiophosphoric acids (Kato et al., 1974; Chauhan et al., 1983; Sowerby et al., 1983). The band shown by the parent acids in the region 2544–2400 cm^{-1}, due to the S-H stretching (Pavia et al., 1996) vibrations, are absent for methylsilane (dialkyl and alkylenedithiophosphate) derivatives, indicating the formation of Si-S which appeared as new bands (Kato et al., 1974) in the region 440–402 cm^{-1}. Two bands of strong intensities present in the region 1099–974 cm^{-1} and 889–810 cm^{-1} may be assigned to ν (P)-O-C and ν P-O-(C) vibrations, respectively (Corbridge, 1969). A band in the region 940–910 cm^{-1} is most probably due to dioxaphospholane and dioxaphosphorinane ring vibrations (Ohkaku and Nakamoto, 1973; Lockhart and Manders, 1986). A sharp band present in the region 684–630 cm^{-1} can be assigned to νP=S vibrations (Drew et al., 1983). Bands with medium intensities in the region 580–505 cm^{-1} may be attributed to vibration of νP-S asymmetric and symmetric vibrations (Gupta et al., 1984). The Si-Cl modes are observed as medium intensity peaks in the narrow range of 330–308 cm^{-1} (Ohkaku and Nakamoto, 1973). Details regarding the individual peaks have been included in Table 2.

^1H NMR spectra

The ^1H-NMR spectra of the MeSi dialkyl and alkylenedithio derivatives were recorded in $CDCl_3$ solution at room temperature. The data for these complexes were similar to those of the corresponding dithiophosphoric acids (Chauhan et al., 1983; Lockhart and Manders, 1986). The Si-methyl protons in MeSi derivatives of dialkyl and alkylene dithiophosphates appear as singlets at ∂ 0.08 ppm. The singlet peak at 4.2–5.1 ppm in the parent dithiophosphoric acids

Table 1: Physical data of methylsilicon (dialkyl and alkylenedithiophosphate) derivatives.

S. no.	Compound formula	Physical state	Molecular weight Found/Cal.	%Si Found/Cal.	%S Found/Cal.	%C Found/Cal.	%H Found/Cal.	%Cl Found/Cal.
1	$MeSi[(EtO)_2PS_2]_3$	Yellow oily liquid	597.21/598.79	4.55/4.69	32.12/32.12	26.45/26.07	5.49/5.55	/00
2	$MeSi(n\text{-}PrO)_2PS_2]Cl_2$	Yellow oily liquid	321.67/327.30	8.48/8.58	19.93/19.59	24.98/25.68	5.67/5.23	20.79/21.66
3	$MeSi[(n\text{-}PrO)_2PS_2]_2Cl$	Yellow oily liquid	505.34/505.12	5.65/5.56	24.68/25.39	30.63/30.90	5.68/6.10	7.48/7.01
4	$MeSi[(n\text{-}PrO)_2PS_2]_3$	Yellow oily liquid	683.57/682.95	4.64/4.11	27.86/28.17	33.93/33.41	6.86/6.64	/00
5	$MeSi[(i\text{-}PrO)_2PS_2]Cl_2$	Yellow oily liquid	325.31/327.30	8.59/8.58	19.27/19.59	25.17/25.68	5.45/5.23	21.64/21.66
6	$MeSi[(i\text{-}PrO)_2PS_2]_2Cl$	Yellow oily liquid	504.82/505.12	5.75/5.56	25.74/25.39	31.27/30.90	6.63/6.10	6.83/7.01
7.	$MeSi[(i\text{-}PrO)_2PS_2]_3$	Yellow oily liquid	683.59/682.95	4.58/4.11	28.43/28.17	33.64/33.41	6.25/6.64	/00
8.	$MeSi[(i\text{-}BuO)_2PS_2]Cl_2$	Yellow oily liquid	352.18/355.35	7.93/7.90	18.34/18.04	30.29/30.41	5.74/5.95	19.52/19.95
9.	$MeSi[(i\text{-}BuO)_2PS_2]_2Cl$	Yellow oily liquid	560.51/561.23	4.68/5.00	22.73/22.85	35.83/36.38	7.27/7.00	6.73/6.31
10.	$[MeSi(i\text{-}BuO)_2PS_2]_3$	Yellow oily liquid	765.73/767.11	3.46/3.66	24.79/25.07	39.63/39.14	7.15/7.48	/00
11.	$MeSi[(PhO)_2PS_2]Cl_2$	Yellow oily liquid	396.42/395.33	7.34/7.10	16.64/16.22	38.83/39.49	3.52/3.31	17.73/17.93
12.	$MeSi[(PhO)_2PS_2]_2Cl$	Yellow oily liquid	640.84/641.19	4.74/4.38	20.8/20.00	46.59/46.82	3.29/3.61	5.62/5.52
13.	$MeSi[(PhO)_2PS_2]_3$	Yellow oily liquid	886.93/887.05	3.27/3.16	21.28/21.68	49.63/50.09	3.57/3.74	/00
14.	$MeSi[S_2POCMe_2CMe_2O]Cl_2$	Yellow oily liquid	326.17/325.28	8.60/8.63	19.47/19.71	25.62/25.84	4.22/4.64	22.39/21.79
15.	$MeSi[S_2POCMe_2CMe_2O]Cl$	Yellow oily liquid	502.48/501.09	5.69/5.60	25.18/25.59	31.57/31.15	5.82/5.43	7.37/7.07
16.	$MeSi[S_2POCMe_2CMe_2O]_3$	Yellow oily liquid	674.24/676.90	4.57/4.14	28.85/28.42	34.19/33.71	5.75/5.80	/00
17.	$MeSi[S_2POCH_2CMe_2CH_2O]_2Cl$	Yellow oily liquid	475.75/473.04	5.82/5.93	27.92/27.11	27.83/27.92	4.74/4.90	7.84/7.49
18.	$MeSi[S_2POCH_2CMe_2CH_2O]Cl_2$	Yellow oily liquid	301.20/311.26	8.54/9.02	20.05/20.60	22.09/23.15	3.89/4.20	22.23/22.78
19.	$MeSi[S_2POCH_2CMe_2CH_2O]_3$	Yellow oily liquid	625.34/634.82	4.11/4.42	29.56/30.30	28.79/30.27	5.07/5.23	00
20.	$MeSi[S_2POCH_2CEt_2CH_2O]_2Cl$	Yellow oily liquid	523.87/529.15	4.96/5.30	23.54/24.23	33.76/34.04	4.56/5.90	5.43/6.70

Table 2: IR spectroscopic data (cm^{-1}) of methylsilicon (dialkyl and alkylenedithiophosphate) derivatives.

S. no.	Compound	ν(P)-O-C	νP-O-(C)	Ring vibration	νP=S	νP-S	ν (Si-S)	ν (Si-Cl)
1	$MeSi[(EtO)_2PS_2]_3$	974 m	889 m	–	651 m	542 m	402 m	
2	$MeSi(n\text{-}PrO)_2PS_2]Cl_2$	990 s	820 s	–	650 m	532 m	413 w	314 m
3	$MeSi[(n\text{-}PrO)_2PS_2]_2Cl$	1099 m	820 s	–	670 s	513 w	422 w	312 m
4	$MeSi[(n\text{-}PrO)_2PS_2]_3$	1056 s	815 m	–	684 m	505 m	410 w	–
5	$MeSi[(i\text{-}PrO)_2PS_2]Cl_2$	1020 s	830 m	–	660 m	530 m	407 m	310 m
6	$MeSi[(i\text{-}PrO)_2PS_2]_2Cl$	1010 s	858 s	–	661 m	540 m	405 m	314 m
7	$MeSi[(i\text{-}PrO)_2PS_2]_3$	1055 s	810 s	–	655 m	543 m	440 w	–
8	$MeSi[(i\text{-}BuO)_2PS_2]\ Cl_2$	1015 m	850 m	–	630 m	542 m	402 m	315
9	$MeSi[(i\text{-}BuO)_2PS_2]_2Cl$	1079 s	889 m	–	651 m	532 m	413 w	308
10	$[MeSi(i\text{-}BuO)_2PS_2]_3$	1067m	820 s	–	650 m	513 w	405 m	–
11	$MeSi[(PhO)_2PS_2]Cl_2$	1020 s	820 s			505 m	440 w	314 m
12	$MeSi[(PhO)_2PS_2]_2Cl$	1010 s	815 m			530 m	402 m	325 m
13	$MeSi[(PhO)_2PS_2]_3$	1055 s	830 m	–		580 m	413 w	–
14	$MeSi[S_2\overline{POCMe_2CMe_2O}]Cl_2$	1145	858 s	940 m	543 m	540 m	405 m	323 m
15	$MeSi[S_2\overline{POCMe_2CMe_2O}]_2Cl$	1010	810 s	923 m	542 m	543 m	440 w	320 m
16	$MeSi[S_2\overline{POCMe_2CMe_2O}]_3$	1143	850 m	912 m	532 m	542 m	402 m	–
17	$MeSi[S_2\overline{POCH_2CMe_2CH_2O}]_2Cl$	1130	889 m	920	513 w	532 m	413 w	318 m
18	$MeSi[S_2\overline{POCH_2CMe_2CH_2O}]Cl_2$	1130	889 m	920	513 w	532 m	413 w	330 m
19	$MeSi[S_2\overline{POCH_2CMe_2CH_2O}]_3$	1056	825	923m	684 m	520 m	412 w	
20	$MeSi[S_2\overline{POCH_2CEt_2CH_2O}]_2Cl$	1150	820 s	910 m	505 m	513 w	405 m	310 m

s, Strong; m, medium; w, weak and b, broad absorption band.

and assigned to SH proton, is absent from the spectra of the new silane complexes indicating deprotonation of SH group and formation of Si-S bond (Gupta et al., 1985).

^{13}C NMR spectra

The ^{13}C NMR spectra were recorded in $CDCl_3$ solution at room temperature. The methyl carbon attached to Si in the methylSi (IV) dithiophosphate complexes were seen in the expected range of 17.8–22.4 ppm. The spectra show very small chemical shifts when compared to those obtained for the parent dithiophosphoric acids and indicate no substantial difference in the structure (Gupta et al., 1984; Srivastava et al., 2010).

^{31}P NMR spectra

As there is only one peak in the proton decoupled ^{31}P NMR, it proves the purity of the complexes formed, and indicates the presence of only one species and also that the three dithiophosphate groups are in identical environments. It has been suggested that the difference in the phosphorus chemical shift between that of the appropriate free acid and the complex is a strong indicator of the mode of binding (Glidewell, 1977). Downfield shifts in the range 9–15 ppm were claimed to be consistent with the presence of bidentate ligands while negligible shifts or even upfield shifts were associated with unidentate linkages. The shift of these peaks related to monodentate mode according to Glidewell (1977). The relevant ^{31}P NMR spectroscopic data of these complexes are given in Tables 3 and 4.

^{29}Si NMR spectra

^{29}Si NMR spectra of some of these complexes have been recorded and the value of ^{29}Si chemical shift falls at −0.21 to −0.83 ppm. These values of chemical shift can be best interpreted in terms of four coordinate silicon in this ligand and derivatives, therefore, behaving as monodentate (Hunter and Reeves, 1968; Elizabeth et al., 1976; Blinka et al., 1984). Thus, based on the above spectroscopic studies, four-coordinate structures may be tentatively proposed for methyl silicon (dialkyl and alkylene dithiophosphate) derivatives.

Table 3: ^1H, ^{31}P, and ^{29}Si NMR spectroscopic data of methylsilicon (dialkyl and alkylenedithiophosphate) derivatives.

S. no.	Compound	^1H chemical shift δ (ppm) in $CDCl_3$	^{31}P chemical shift	^{29}Si chemical shift
1	$MeSi[(EtO)_2PS_2]_3$	0.08, s, 3H, MeSi 1.39 (t, $J=6$Hz, 6H, $3\times CH_3$; 4.33 (q, $J=6$ Hz, 4H, $2\times CH_2$)	86.7	−0.22
2	$MeSi\ (n\text{-}PrO)_2PS_2]Cl_2$	0.08, s, 3H, MeSi 1.10 (t, $J=5.8$ Hz, 6H, $2\times CH_3$), 1.84 (m, 4H, $2\times CH_2$); 4.27 ($J=5.3$ Hz, 4H, $2\times CH_2$)	87.4	−0.83
3	$MeSi[(n\text{-}PrO)_2PS_2]_2Cl$	0.08, s, 3H, MeSi 1.10 (t, $J=5.8$ Hz, 12H, $4\times CH_3$), 1.84 (m, 8H, $4\times CH_2$); 4.27 ($J=5.3$ Hz, 8H, $4\times CH_2$)	86.8	−0.61
4	$MeSi[(n\text{-}PrO)_2PS_2]_3$	0.08, s, 3H, MeSi 1.08 (t, $J=5.8$ Hz, 18H, $6\times CH_3$), 1.84 (m, 12H, $6\times CH_2$); 4.25 ($J=5.3$ Hz, 12H, $6\times CH_2$)	85.9	
5	$MeSi[(i\text{-}PrO)_2PS_2]Cl_2$	0.08, s, 3H, MeSi 1.52 (d, $J=5.5$ Hz, 6H, $2\times CH_3$); 4.90 (m, 1H, CH)	83.5	
6	$MeSi[(i\text{-}PrO)_2PS_2]_2Cl$	0.08, s, 3H, MeSi 1.52 (d, $J=5.5$ Hz, 12H, $4\times CH_3$); 4.90 (m, 2H, $2\times CH$)	84.1	
7	$MeSi[(i\text{-}PrO)_2PS_2]_3$	0.08, s, 3H, MeSi 1.52 (d, $J=5.5$ Hz, 18H, $6\times CH_3$); 4.90 (m, 3H, $3\times CH$)	82.7	
8	$MeSi[(i\text{-}BuO)_2PS_2]Cl_2$	0.08, s, 3H, MeSi 0.98 (d, $J=3.6$ Hz, 6H, $2\times CH_3$); 2.0 (m, 1H, CH); 4.05 (d, $J=6.4$ Hz, 2H, CH_2)	86.2	
9	$MeSi[(i\text{-}BuO)_2PS_2]_2Cl$	0.08, s, 3H, MeSi	85.7	
10	$[MeSi(i\text{-}BuO)_2PS_2]_3$	0.08, s, 3H, MeSi 0.98 (d, $J=3.6$ Hz, 18H, $6\times CH_3$); 2.0 (m, 3H, $3\times CH$); 4.05 (d, $J=6.4$ Hz, 6H, $3\times CH_2$)	85.9	
11	$MeSi[(PhO)_2PS_2]Cl_2$	0.08, s, 3H, MeSi, 7.26 (m, ArH)	79.3	
12	$MeSi[(PhO)_2PS_2]_2Cl$	0.08, s, 3H, MeSi, 7.28 (m, ArH)	80.5	
13	$MeSi[(PhO)_2PS_2]_3$	0.08, s, 3H, MeSi, 7.24 (m, ArH)	78.6	
14	$MeSi[S_2POCMe_2CMe_2O]Cl_2$	0.08, s, 3H, MeSi, 1.62 (s, 12H, $4\times CH_3$)	93.2	−0.81
15	$MeSi[S_2POCMe_2CMe_2O]_2Cl$	0.08, s, 3H, MeSi, 1.60 (s, 24H, $8\times CH_3$)	93.4	−0.53
16	$MeSi[S_2POCMe_2CMe_2O]_3$	0.08, s, 3H, MeSi, 1.62 (s, 36H, $12\times CH_3$)	94.1	−0.21
17	$MeSi[S_2POCH_2CMe_2CH_2O]_2Cl$	0.08, s, 3H, MeSi 4.10, d, 8H(OCH_2), $J(PH)=15.6$ Hz 1.12, s, 12H(CH_3)	78.61	
18	$MeSi[S_2POCH_2CMe_2CH_2O]Cl_2$	0.08, s, 3H, MeSi 4.12, d, 4H(OCH_2), $J(PH)=15.5$ Hz 1.11, s, 6H(CH_3)	80.42	
19	$MeSi[S_2POCH_2CMe_2CH_2O]_3$	0.08, s, 3H, MeSi 4.12, d, 12H(OCH_2), $J(PH)=15.5$ Hz 1.12, s, 18H(CH_3)	79.56	
20	$MeSi[S_2POCH_2CEt_2CH_2O]_2Cl$	0.08, s, 3H, MeSi 0.71, t ($J=7.5$ Hz),12H(CH_3), 1.11, q ($J=7.5$ Hz), 8H(CH_2) 4.02, d, 8H(OCH_2), $J(PH)=16$ Hz	79.0	

[a]Solvent used is $CDCl_3$.

Structural elucidation

IR, NMR (^1H, ^{13}C, ^{31}P, and ^{29}Si), molecular weight determination, and elemental analyses indicate that the ligand is a monodentate ligand. The observed ^{29}Si also confirms the tetrahedral environment about the silicon atom in which the ligand moieties are bonded through monodentate ester type linkage.

Table 4: ^{13}C NMR spectroscopic data of of methylsilicon (dialkyl and alkylenedithiophosphate) derivatives.

S. no	Compound	^{13}C chemical shift (ppm)					
		CH_3	CH_2	CH	C	CO	MeSi
1	$MeSi[S_2P(OEt)_2]_2Cl$	15.9 s				63.3 s	17.8 s
2	$MeSi[S_2P(OPr\text{-}i)_2]_2Cl$	23.1 s				72.4 s	22.4 22.0 d
3	$MeSi[S_2\overline{POCH_2CMe_2CH_2O}]_2Cl$	19.8 21.3 t			32.9s	77.0 77.1 d	18.9 s

s, Singlet; d, doublet; t, triplet.

Antimicrobial activity of dithiophosphate derivatives of silane

The bioactivity of silane complexes was evaluated against one Gram-negative bacterium *Escherichia coli* and one Gram-positive bacterium *Staphylococcus aureus*. The microbiological media used in the study were supplied by Becton, Dickinson and Company (Franklin Lakes, NJ, USA). Antibacterial activity analysis was assessed using Bioscreen C (Automated Microbiology Growth Analysis System) manufactured in Finland by OY Growth Curves CE. The bacteria were purchased at American Type Culture Collection (ATCC) (Manassas, VA, USA). Instruments used were iS10 FT-IR (Thermoscientific) and an Anasazi eft-90 NMR instrument. All chemicals from Sigma-Aldrich (St. Louis, MO, USA). The Bioscreen C measures microorganism growth. As microorganisms grow, they increase the turbidity of their growth medium. An optical density (OD) curve is generated from the turbidity measurement of growth medium over time, and the curve indicates the growth of the bacterium. In other terms, the degree of turbidity in broth culture is directly related to the number of microorganism present, either viable or dead cells, and is a rapid method of measuring cell growth rate of an organism. The amount of transmitting light through turbid broth decreases with subsequent increase in the absorbance value.

In order to study bacterial growth in broth culture, 4–5 mL of bacterial culture were placed in 200 mL of Bacto Nutrient broth contained in a 250 mL flask. After 24 h, a 1:10 mixture of the 24-h bacterial growth and sterile physiological saline water were prepared. An aliquot of 100 μL from each solution was placed into different wells of the Bioscreen C. The first column wells served as controls and had silane complexes. Aliquots of 50 μL of the silane derivative solution were added to the samples. The growth rate was determined by measuring turbidity using the Bioscreen C for a total of 24 h at regular intervals (30 min).

An OD curve was generated based on the turbidity measurement over a period of 24 h. During the experiment, the data were exported to a PC in MS Excel. Microbiological calculations were generated directly to MS Excel sheets automatically. Measurements were then processed to generate microbiological growth curves, plotting turbidity vs. time (Abu-Basha et al., 2012).

The *E. coli* bacterial growth curve is normal with a short lag phase followed by a rapid bacterial growth up to 300 min. Then, the rate of growth slows down due to inhibition of further cell division; accumulation of dead cells at the bottom of the well. This leads to accumulation of waste which is going to be used by hiding, living cells, and this is illustrated by the bacterial growth picking up at around 600 min. The bacterial growth of *S. aureus* is normal while the lag phase is absent. This could be due to the microorganism from a nutritionally poor medium which is added to a nutritionally rich medium; it can simply adapt to the environment and starts the cell division with no delay, and, therefore, lag phase may be absent. The bacterium grows rapidly up to 300 min, then seems to lose its ability to reproduce and begins to die quickly and goes to the bottom. Usually, the depletion of nutrients and the subsequent accumulation of metabolic waste products in the broth facilitate the bacterial death phase, but in this case, almost immediately the bacteria began to grow again and the number of bacteria increases exponentially, which is probably due to the number of live cells exceeding the number of dead cells. In addition, *S. aureus* is a hardy bacterium which survives in the highest salt conditions. Also, the strain-to-strain variation should be considered in growth rates.

The overall results indicated that silane complexes showed antibacterial activity at a concentration of 50 μL of silane derivative treatment to 100 μL of the bacterial solution towards the Gram-positive and Gram-negative test bacteria. The antibacterial activity of selected silane compounds using acid derivatives was found to exert inhibitory effects on *E. coli* and *S. aureus*.

Methylsilane compounds like $\mathrm{MeSi[S_2P(}$*i*$\mathrm{\text{-}BuO)_2]Cl_2}$, $\mathrm{MeSi[S_2P(}$*i*$\mathrm{\text{-}BuO)_2]_3}$, $\mathrm{MeSi[S_2POCH_2CMe_2CH_2O]_2Cl}$, $\mathrm{MeSi[S_2POCH_2CMe_2CH_2O]Cl_2}$, $\mathrm{MeSi[S_2POCH_2CMe_2CH_2O]_3}$, and $\mathrm{MeSi[S_2P(}$*n*$\mathrm{\text{-}PrO)_2]_3}$ have been added to both strains at the same concentration. All inhibited the growth of *E. coli* and *S. aureus* based on the OD readings as compared to the control. The control wells without silane complexes showed OD absorption, increase in both bacteria, while the test wells showed OD absorption decrease implying little or no growth. Based on our results, both bacteria appeared to be susceptible to silane complexes which exhibited antibacterial properties. There was a dramatic difference in optical densities of silane complexes at $t = 0$ min in both *E. coli* and *S. aureus* graphs.

Figure 1 shows that the effect of *n*-propyl derivative (1:3) $\mathrm{MeSi[S_2P(}$*n*$\mathrm{\text{-}PrO)_2]_3}$ was rapid, indicating a decrease in turbidity, which translates into a reduction in bacterial activity; *n*-propyl derivative displays the most dramatic change in turbidity during the first 4 h and levels off in constant turbidity up to 24 h. Neopentylene derivative (1:1) $\mathrm{MeSi[OCH_2CMe_2CH_2OPS_2]Cl_2}$ shows a slow effect on *E. coli*, while maintaining a relatively high turbidity during 24 h compared to *n*-propyl derivative (1:3). Neopentylene derivative (1:3) $\mathrm{MeSi[S_2POCH_2CMe_2CH_2O]_3}$, isobutyl derivative (1:3) $\mathrm{MeSi[S_2P(}$*i*$\mathrm{\text{-}BuO)_2]_3}$, and isobutyl derivative (1:1) $\mathrm{MeSi[S_2P(}$*i*$\mathrm{\text{-}BuO)_2]Cl_2}$ showed an immediate, significant, and sustained reducing effect on *E. coli*. While it still has an inhibitory effect, neopentylene derivative (1:2) $\mathrm{MeSi[OCH_2CMe_2CH_2OPS_2]_2Cl}$ shows a higher bacterial growth.

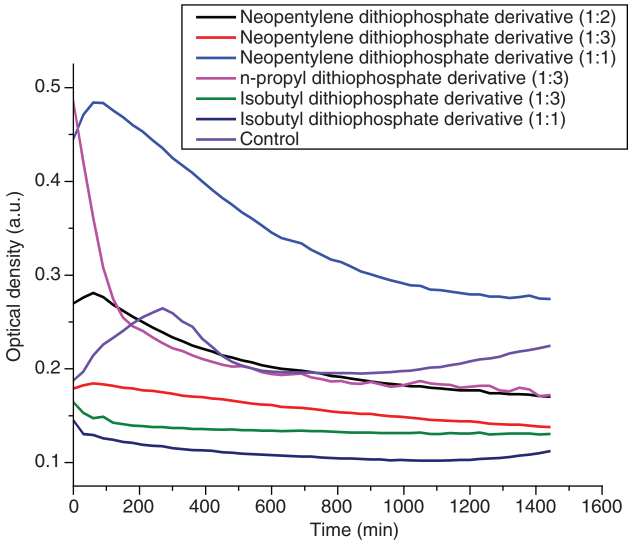

Figure 1: Antimicrobial effect of dithiophosphate derivatives on *Escherichia coli*.

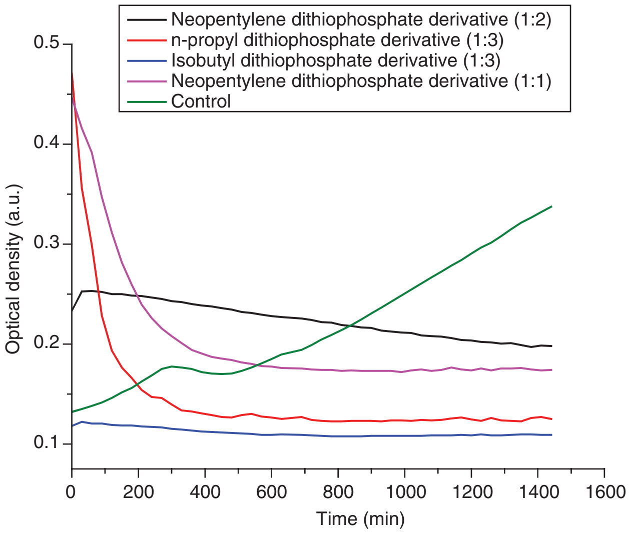

Figure 2: Antimicrobial effect of dithiophosphate derivatives on *Staphylococcus aureus*.

On the other hand, while the untreated *S. aureus* (control) has an increased bacterial activity during 24 h (Figure 2), *n*-propyl derivative (1:3) and neopentylene derivative (1:1) had an immediate, significant and sustained effect on *S. aureus*; the OD decreases relatively quickly, reaches a bottom and levels off. Neopentylene derivative (1:2) and isobutyl derivative (1:3) had an immediate and sustained effect on *S. aureus* compare to *n*-propyl derivative (1:3) and neopentylene derivative (1:1) with isobutyl derivative (1:3) having a greater inhibiting effect. Based on our knowledge, this dramatic difference in OD could be related to the chemical structure of these compounds. We believe, based on these preliminary findings, straight chains (*n*-propyldithiophosphate) have higher OD than the cyclic chains (neopentylenedithiophosphate) followed by branched chains (*n*-isobutyldithiophosphate) with the lowest OD. Further studies need to be done in order to explore the relationship between dithiophosphate derivatives structure and the sample turbidity.

Similar results were obtained in previous studies where dithiophosphoric acid and their O, O-dialkyl and alkylene dithiophosphate bis(cyclopentadienyl)-zirconium (IV) hydride complexes exerted an antibacterial effect on *E. coli* and *S. aureus* (Elkhaldy et al., 2011). Also Elkhaldy et al. (2012) reported that *bis* (neopentylene dithiophosphoric acid) adducts of diphenyl diselenide had a higher antibacterial activity than *bis* (2, 2-diethyl propane-1, 3-diol dithiophosphoric acid) adduct of diphenyl diselenide on *S. aureus* (Gram-positive) and *E. coli* (Gram-negative) bacteria at different concentrations of the two adducts. The difference in OD of the dithiophosphate derivatives suggests that saline derivatives of dialkyl and alkylene dithiophosphate are found to be more antibacterial than their parent ligand.

Conclusion

In this study, we have shown the facile synthesis of dialkyl and alkylene dithiophosphate derivatives of silicon. All these new compounds were characterized using ^{1}H, ^{13}C, ^{31}P, ^{29}Si NMR, IR, and elemental analyses. We showed that dialkyl and alkylene dithiophosphoric acids, respectively, their sodium salts react as a monodentate ligand with methyltrichlorosilane. The resulting methyl silicon compounds exhibited higher antimicrobial activity than the dithiophosphate ligands.

Experimental

General procedure

Stoichiometric amounts of methyl-silicon trichloride and the sodium salts of dithiophosphoric acids in benzene were stirred for ~5 h. The clear filtrate was evaporated at low pressure and the resulting oily liquid was dried under vacuum.

Materials: Solvents (benzene, alcohols, dichloromethane and n-hexane, etc.) were dried by standard methods. Glycols were distilled before use. MeSiCl$_3$ and Phosphorous pentasulfide (E. Merck) was used as received. O, O-dialkyl and alkylenedithiophosphoric acids were prepared by the reaction of phosphorus pentasulfide and alcohols in a 1:4 ratio, and in a 1:2 ratio with glycols as described in the literature (Chauhan et al., 1983).

Measurements: The elemental analysis (C and H) was performed on a Perkin-Elmer 2400 elemental analyzer. Sulfur was estimated gravimetrically as barium sulfate. Volhard method was used to estimate chlorine. Silicon was estimated gravimetrically in the oxide form using the (cupferron method). Molecular weights were determined cryoscopically in benzene. Infrared spectra were recorded as Nujol mulls using CsI cells in the region 4000–200 cm^{-1} on an iS10 FT-IR spectrophotometer. ^{1}H and ^{13}C spectra were recorded on a Anasazi eft-90 and using TMS as the internal reference. ^{31}P NMR spectra were recorded in CDCl$_3$ using H$_3$PO$_4$ as an external reference on the same instrument.

Preparation

Reaction of MeSiCl$_3$ with sodium diethyldithiophosphate in 1:3 molar ratio: An exothermic reaction occurred when solid sodium diethyldithiophosphate (1.93 g, 9.28 mmol) was added to a benzene solution (~70 mL) of MeSiCl$_3$ (0.46 g, 3.09 mmol). The reaction mixture was refluxed for ~5 h to ensure the completion of the reaction. The precipitate of NaCl (0.51 g) was filtered out and the removal of the solvent from the filtrate under reduced pressure and anhydrous conditions yielded MeSi[S$_2$P(OEt)$_2$]$_3$ (1.77 g, 95% yield). The yellow oily compound MeSi[S$_2$P(OEt)$_2$]$_3$ was purified by repeated washing with dried n-hexane (Table 1).

Acknowledgments: This work has been supported in part by Evans Allen Federal appropriated fund.

References

Abu-Basha, E. A.; Gharaibeh, S. M.; Thabet, A. M. In vitro susceptibility of resistant, *Escherichia coli* field isolates to antimicrobial combinations. *J. Appl. Poultry Res.* **2012**, *21*, 595–602.

Blinka, T. A.; Helmer, B. J.; West, R. Polarization transfer NMR spectroscopy for silicon-29: the INEPT and DEPT techniques. *Adv. Organomet. Chem.* **1984**, *23*, 193–218.

Chauhan, H. P. S.; Bhasin, C. P. G.; Srivastava, G.; Mehrotra, R. C. Synthesis and characterization of 2-mercapto-2-thiono-1, 3, 2-dioxaphospholanes and dioxaphosphorinanes. *Phosporus Sulfur Silicon Relat. Elem.* **1983**, *15*, 99–104.

Corbridge, D.E.C. The Infrared Spectra of Phosphorus Compounds. In *Topics in Phosphorus Chemistry*, John Wiley & Sons: New York, 1969; Vol. 6, pp. 235–366.

Cotero-Villegas, A. M.; García y García, P.; Höpfl, H.; Pérez-Redondo, M. C.; Martínez-Salasb, P.; López-Cardosob, M.; Cea-Olivares R. Synthesis and multinuclear (1H, 13C, 31P, 119Sn) NMR study of trimethyl and triphenyl-tin (IV) with cyclic dithiophosphate ligands. *J. Organomet. Chem.* **2011**, *696*, 2071–2078.

Drew, M. G. B.; Baricalli, P. J.; Mitchell, P. C. H.; Read, A. R. Crevice coordination: binding of a ligand molecule in a molecular crevice. Crystal and molecular structures of μ-oxo-μ-pyridine-μ-sulphido-bis [(O, O′-di-isopropyl phosphorodithioato)oxo- molybdenum (V)] and μ-oxo-μ-pyridazine-μ-sulphido-bis[(O, O′-di-isopropyl phosphorodithioato) oxomolybdenum(V)]. *J. Chem. Soc. Dalton Trans.* **1983**, 649–655. doi: 10.1039/DT9830000649.

Elizabeth A. W.; Joseph D. C.; Ronald W. L. Silicon-29 NMR. Solvent effects on chemical shifts of silanols and silylamines. *J. Organomet. Chem.* **1976**, *108*, 153–158.

Elkhaldy, A. A. S.; Abushanab, A. M.; Abu Alkhair, E. Synthesis and antimicrobial studies of bis (O, O′-dialkyl and alkylene dithiophosphoric acids) adducts of diphenyl diselenide. *Appl. Organomet. Chem.* **2011**, *25*, 487–595.

Elkhaldy, A. A. S.; Hussien, A. R.; Abushanab, A. M.; Wassef, M. A. Synthesis, spectroscopic, and antimicrobial studies on O, O′-dialkyl and alkylene dithiophosphate cyclopentadienyl-zirconium (IV) hydride. *J. Sulfur Chem. First.* **2012**, *33*, 295–302.

García y García, P.; Martínez-Salasb, P.; Hernández-Ortega, S.; Román- Bravo, P.; López-Cardoso, M.; Pérez-Redondo, M. C.; Vargas-Pineda, G.; Cotero-Villegas, A.M.; Cea-Olivares, R. Synthesis, structure and characterization of new stibocanes substituted with dithiophosphate ligands. *Polyhedron* **2012**, *37*, 48–53.

Glidewell, C. Ambident nucleophiles: VI. Solution metal-ligand binding modes in phosphorodithioate complexes. A phosphorus-31 N.M.R. study. *Inorg. Chim. Acta* **1977**, *25*, 159–163.

Gupta, R. K.; Rai, A. K.; Mehrotra, R. C.; Jain, V. K. Cyclic O, O-alkylenedithiophosphates of phenyl-arsenic and -antimony. *Inorg. Chim. Acta* **1984**, *88*, 201–207.

Gupta, R. K.; Rai, A. K.; Mehrotra, R. C.; Jain, V. K.; Hoskins, P. F.; Tiekink, E. R. T. Phenylarsenic(III) and phenylantimony(III) bis(dialkyl dithiophosphates): synthesis and multinuclear (proton, carbon-13, phosphorus-31) NMR and mass spectral studies. Crystal and molecular structures of $C_6H_5M[S_2P(OCHMe_2)_2]_2$ [M = Sb(III) and As(III)]. *Inorg. Chem.* **1985**, *24*, 3280–3284.

Hunter, B. K.; Reeves, L. W. Chemical shifts for compounds of the group IV elements silicon and tin. *Can. J. Chem.* **1968**, *46*, 1399–1414.

Kato, S.; Hori, A.; Shiotani, H.; Mizuta, M.; Hayashi, N.; Takakuwa, T. Infrared and Raman spectra of (thioacetoxythio) triorgano derivatives of silicon, germanium, tin and lead. *J. Organomet. Chem.* **1974**, *82*, 223–228.

Kaub, C.; Augenstein, T.; Bauer, T. O.; Rothe, E.; Es mezjan, L.; Schünemann, V.; Roesky, P. W. High-coordinate gold (I) complexes with dithiocarboxylate ligands. *Inorg. Chem.* **2014**, *53*, 4491–4499.

Kim, B.; Mourhatch, R.; Aswath, B.P. Properties of tribofilms formed with ashless dithiophosphate and zinc dialkyl dithiophosphate under extreme pressure conditions. *Wear* **2010**, *268*, 579–591.

Lockhart, T. P.; Manders, W. P. Structure determination by NMR Spectroscopy. Dependence of |2J (119Sn, 1H) on the Me-Sn-Me Angle in methyltin(IV) compounds. *Inorg. Chem.* **1986**, *25*, 892–895.

Lutz, T.; MacLachlan, A.; Sudlow, A.; Nelson, J.; Michael, S. H.; Kieran, C.; Molloy, K. C.; Haque, S. A. Thermal decomposition of solution processable metal xanthates on mesoporous titanium dioxide films: a new route to quantum-dot sensitised heterojunctions. *Phys. Chem. Chem. Phys.* **2012**, *14*, 16192–16196.

Ma, N.; Li, Y.; Xu, H.; Wang, Z.; Zhang, X. Well-defined, reversible boronate crosslinked nanocarriers for targeted drug delivery in response to pH and cis-diols. *J. Am. Chem. Soc.* **2010**, *132*, 442–443.

Ohkaku, N.; Nakamoto, N. Metal isotope effect on metal-liquid vibrations. X. Far-infrared spectra of trans adducts of tin (IV) tetrahalide with unidentate ligands. *Inorg. Chem.* **1973**, *12*, 2440–2446.

Pavia, D. L.; Lampman, G. M.; Kris, G. S. Introduction to Spectroscopy; 2nd Edition. Saunders Golden Sunburst Series: Orlando, 1996.

Petrus, H. T. B. M.; Hirajima, T.; Sasaki, K.; Okamoto, H. Effect of pH and diethyl dithiophosphate (DTP) treatment on chalcopyrite and tennantite surface observed using atomic force microscopy (AFM). *Colloids Surf. Physicochem. Eng. Aspects* **2011**, *9*, 266–273.

Rodina, A. T.; Korneeva, V. E.; Antzutkin N. O.; Ivanov, V. A. Supramolecular self-organisation and conformational isomerism of abinuclear O, O-dipropyl dithiophosphate gold(I) complex, $[Au_2\{S_2P(OC_3H_7)_2\}_2]$: synthesis, 13C and 31P CP/MAS NMR spectroscopy, single-crystal X-ray diffraction study and thermal behaviour. *Spectrochim. Acta Part A Mol. Biomol. Spectrosc.* **2015**, *149*, 881–888.

Sowerby, D. B.; Haiduc, I.; Barbul-Rusu, A.; Salajan, M. Antimony (III) diorganophosphoro- and diorganophospinodithioates: crystal structure of Sb $[S_2P(OR)_2]_3$ (R = Me and i-Pr). *Inorg. Chim. Acta* **1983**, *162*, 87–96.

Srivastava, S. K.; Tomar, S.; Rastogi, R.; Saxena, R. Substituted diorganotin (IV) O, O′-alkylene dithiophosphates: synthesis and spectral aspects. *Phosphorus Sulfur Silicon Relat. Elem.* **2010**, *185*, 634–640.

Zhao, F.; Kasrai, M.; Sham, T. K.; Bai, Z.; Zhao, D. Characterization of tribofilms derived from zinc dialkyl dithiophosphate and serpentine by X-ray absorption spectroscopy. *Tribol. Int.* **2014**, *73*, 167–176.